

## Appendix B: Equilibrium and stability analysis.

We assessed local stability of the point equilibrium by linearizing the dynamic equations (Eqs. 1–2) to find the characteristic equation. We obtained numerical solutions for the roots using the 'multiroot' function in the 'rootSolve' package in the R software version 3.1.1 (Soetaert 2009, R Core Team 2014). We conducted tests of the stability boundaries with numerical integration using the 'Solv95' software (Wood 1999). Where the point equilibrium was locally unstable, our numerical solutions showed that perturbations led to stable limit cycles.

Here we present additional results to facilitate comparison of models with and without demographic heterogeneity. First we show that the qualitative pattern for the equilibrium density and maturation delay is identical for all values of  $\theta_q$  between  $\theta_q=0.5$  and  $\theta_q=1$  (Fig. B1). In particular, increasing settlement rate ( $S$ ) causes the equilibrium adult density ( $N_a^*$ ) to increase then decrease, while the maturation delay ( $\tau_q^*$ ) increases. Over this range of  $\theta_q$ , the equilibrium is locally unstable for intermediate values of  $S$  (Fig. B2; identical to Fig. 2b in main text, and shown here for clarity). Fig. 1 in the main text corresponds to a vertical cross-section through Fig. B1-B2 at  $\theta_q=1$ , i.e., all high quality larvae with  $\theta_h=1$ . In Figs B3-B4 we present additional vertical cross-sections at  $\theta_q=0.5$  (left edge of Fig. 2) and  $\theta_q=0.75$  (center of Fig. 2).

With demographic heterogeneity, the equilibrium adult density and maturation delays for high and low quality types also follow qualitatively similar patterns (Fig. B5, compare to Fig. B1). This qualitative pattern does not depend on whether the equilibrium is stable throughout the range of  $S$  ( $p_h=0.1$ , Fig. B6) or passes through the unstable region ( $p_h=0.5$ , Fig. B7). However, equilibrium stability depends on the quantitative differences. In Fig. B8 we plot the population dynamics after a small perturbation from the equilibrium for  $S=10^3$  with  $p_h=0.1$  (in the stable region) and  $p_h=10^{-6}$  (in the unstable region, see Fig. 2). These time series illustrate the

mechanism by which demographic heterogeneity can stabilize the equilibrium, as described in the Results. For  $p_h=0.1$  (Fig. B8, solid lines), sufficient high quality settlers increase the adult density more rapidly than for  $p_h=10^{-6}$  (Fig. B8a) and suppress juvenile survival (Fig. B8b), thereby dampening the oscillations. With few high quality settlers ( $p_h=10^{-6}$ , dashed lines), cycle amplitude continues to increase and the dynamics approach a stable limit cycle. The minimum and maximum adult densities on the stable limit cycles over the range of  $p_h$  are displayed in Fig. B9.

For low  $S$ , the equilibrium is stable for all values of  $p_h$  including the extremes, where the settlers are nearly homogeneous ( $p_h$  near 0 or 1). This can be seen in Fig. B10, which is the lower portion of Fig. 2a in the main text.

#### LITERATURE CITED

- R Core Team. 2014. R: A language and environment for statistical computing. R Foundation for Statistical Computing, Vienna, Austria. URL <http://www.R-project.org/>.
- Soetaert, K. (2009). rootSolve: Nonlinear root finding, equilibrium and steady-state analysis of ordinary differential equations. R-package version 1.6.
- Wood, S.N. 1999. Solv95: a numerical solver for systems of delay differential equations with switches. URL <http://www.maths.bath.ac.uk/~sw283/simon/dde.html>.

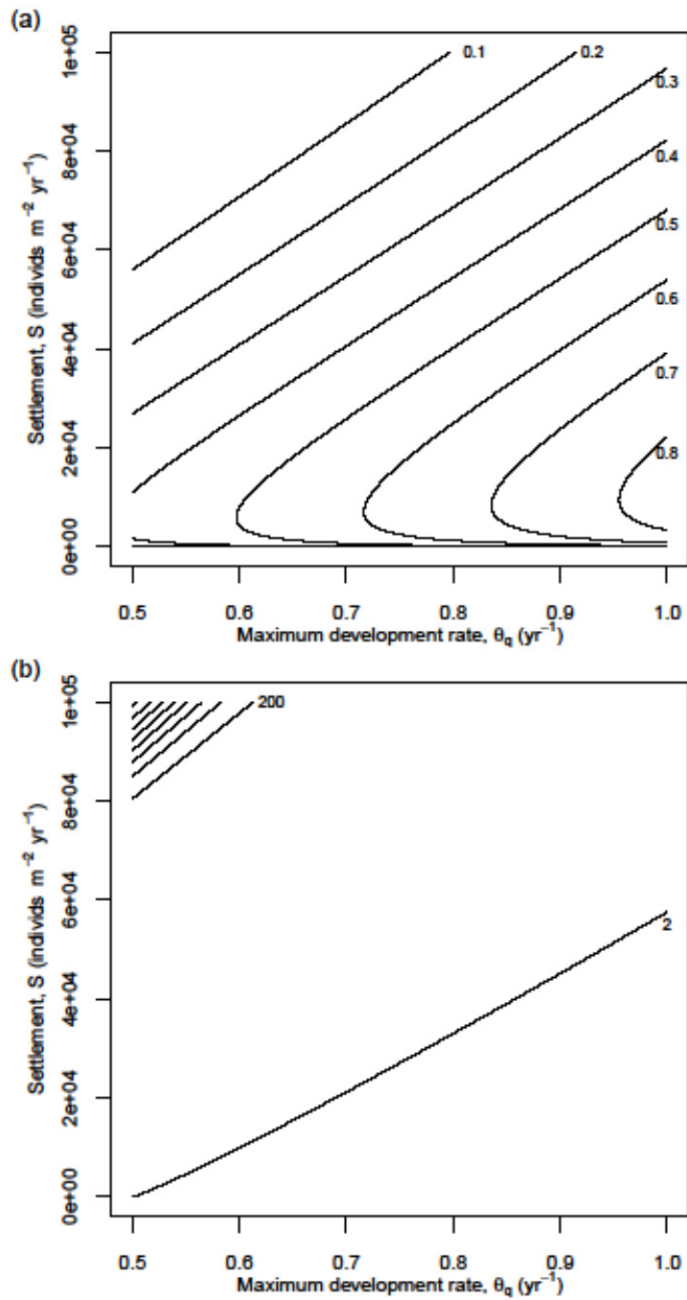


FIG. B1. Contours of equilibrium (a) adult density,  $N_a^*$ , and (b) development delay,  $\tau_q^*$ , as a function of settlement rate and maximum development rate, for the model with homogeneous larvae.

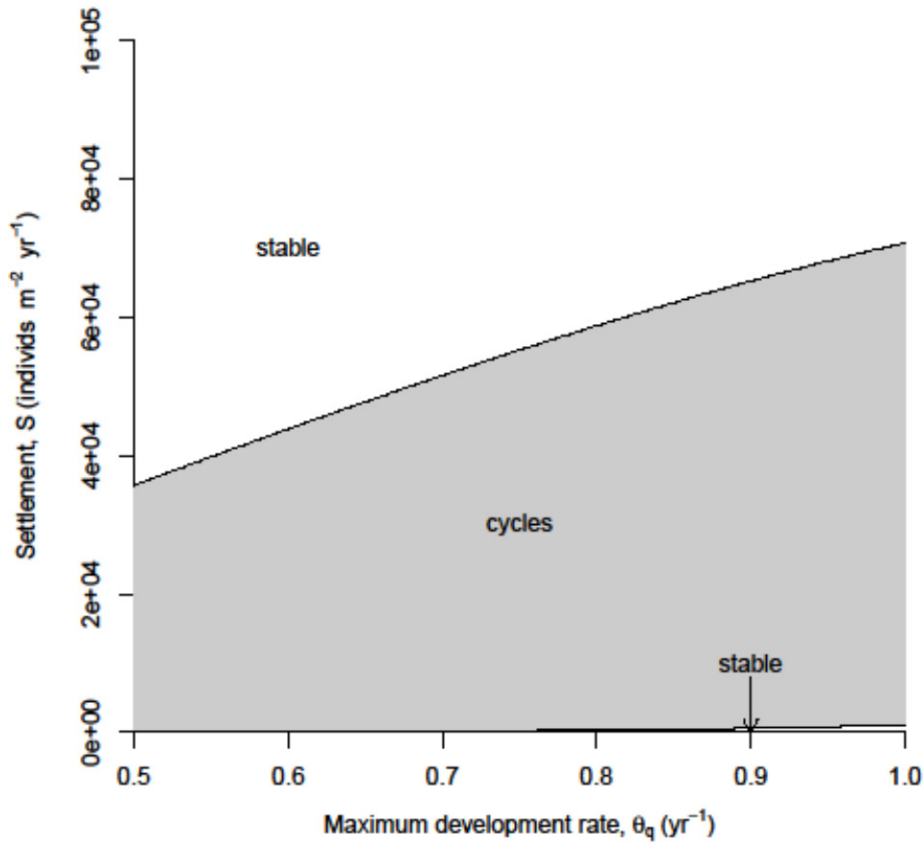


FIG. B2. Stability boundaries for the model with homogeneous larvae. The left and right edges ( $\theta_q=0.5$  and 1, respectively) are identical to the left and right edges of Fig. 2a ( $p_h=0$  and  $p_h=1$ ) in the main text. The equilibrium is stable at low  $S$  for  $0.5 \leq \theta_q \leq 1$ , although the lower boundary is difficult to see on the scale of this graph. At  $\theta_q=0.5$  the equilibrium is stable for  $S < 43$ , and at  $\theta_q=1$  the equilibrium is stable for  $S < 1057$ .

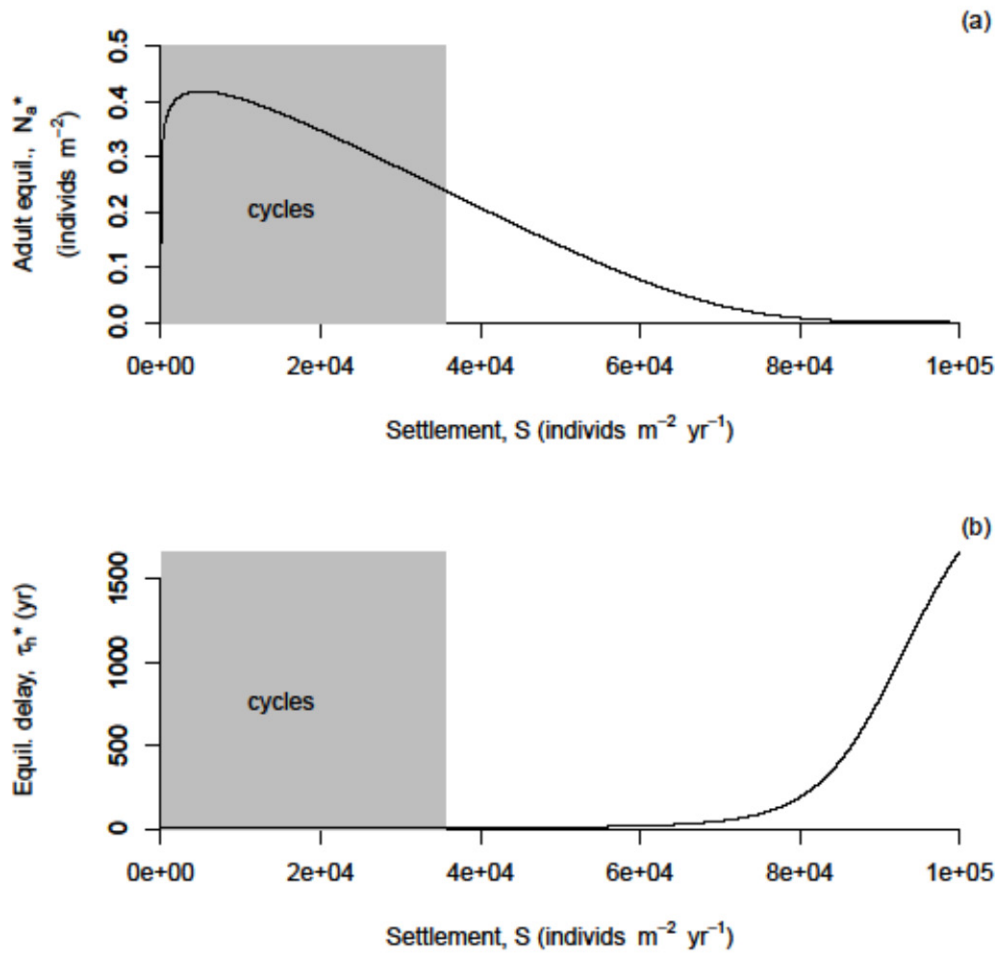


FIG. B3. Equilibrium (a) adult density,  $N_a^*$ , and (b) development delay,  $\tau_q^*$ , for homogeneous larvae with  $\theta_q=0.5$ . This corresponds to a vertical cross-section at the left edge of Figs B1-B2. The model predicts an unstable point equilibrium with stable limit cycles for the range of  $S$  indicated by shading. The equilibrium is stable for larger and smaller values of  $S$  (lower stability boundary is difficult to see on the scale of this graph).

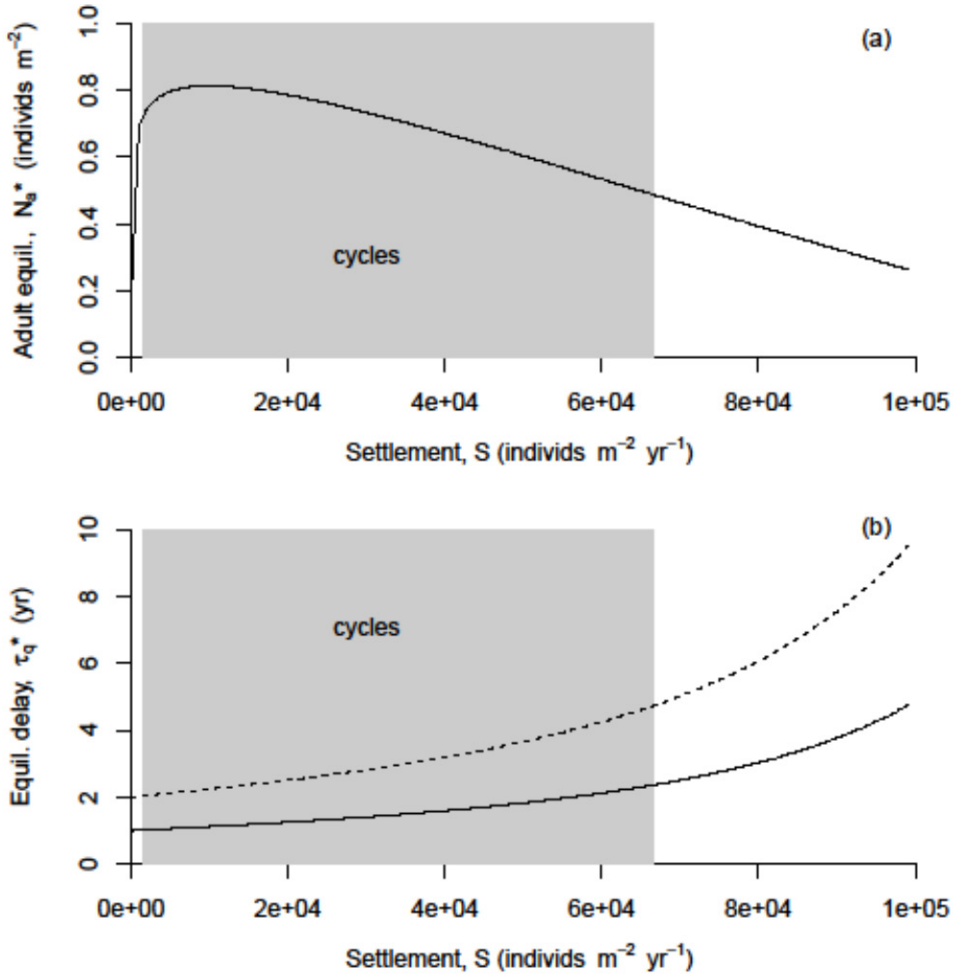


FIG. B4. Equilibrium (a) adult density,  $N_a^*$ , and (b) development delay,  $\tau_q^*$ , for homogeneous larvae with  $\theta_q=0.75$ . This corresponds to a vertical cross-section through the middle of Figs B1-B2. The model predicts an unstable point equilibrium with stable limit cycles for the range of  $S$  indicated by shading. The equilibrium is stable for larger and smaller values of  $S$  (lower stability boundary is difficult to see on the scale of this graph).

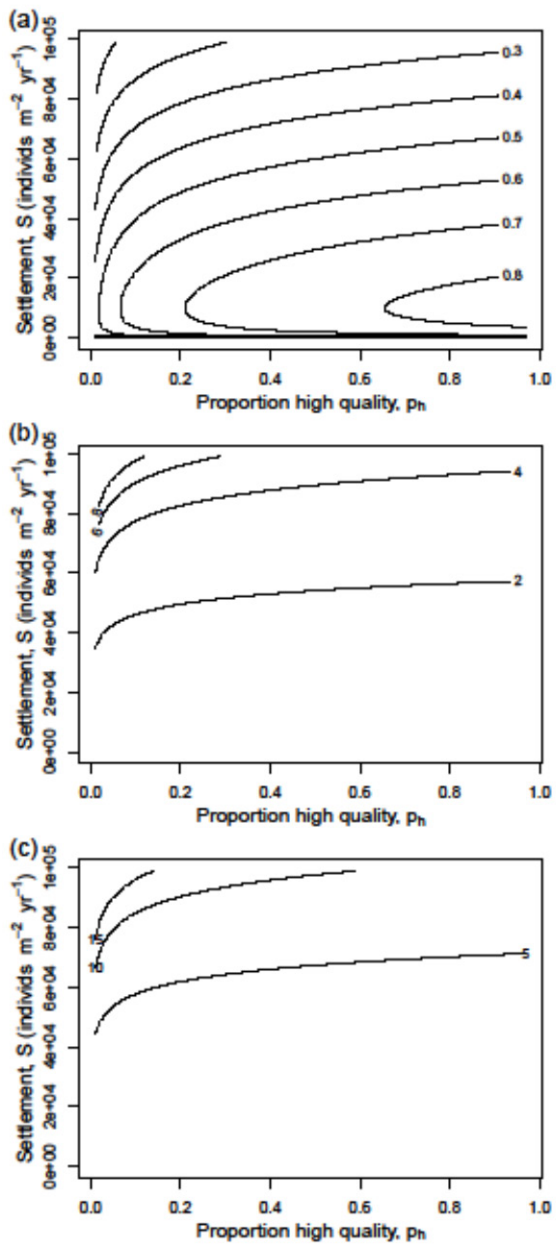


FIG. B5. Contours of equilibrium (a) adult density,  $N_a^*$ , and (b) high quality development delay,  $\tau_h^*$ , and (c) low quality development delay,  $\tau_l^*$ , as functions of settlement rate and proportion high quality larvae, for the model with heterogeneous larvae.

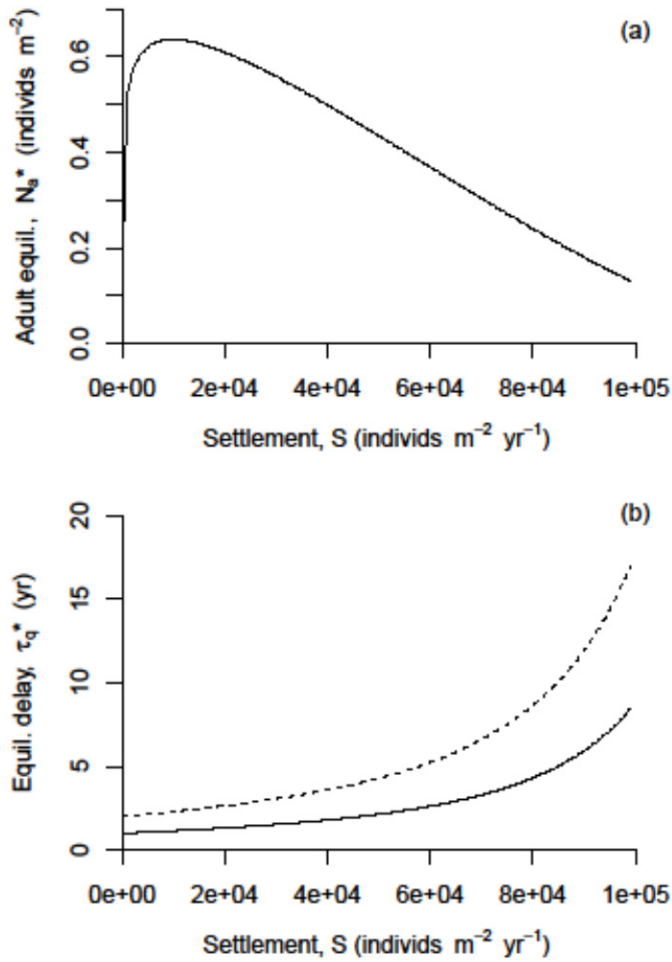


FIG. B6. Equilibrium (a) adult density, and (b) development delay for the model with heterogeneous larvae and  $p_h=0.1$ . In (b), the solid line indicates the delay for high quality larvae ( $\tau_h^*$ ), and the dashed line indicates the delay for low quality larvae ( $\tau_l^*$ ). This plot corresponds to a vertical cross-section through Fig. 2a (in the main text) at  $p_h=0.1$ , where the equilibrium is locally stable for all values of  $S$ .

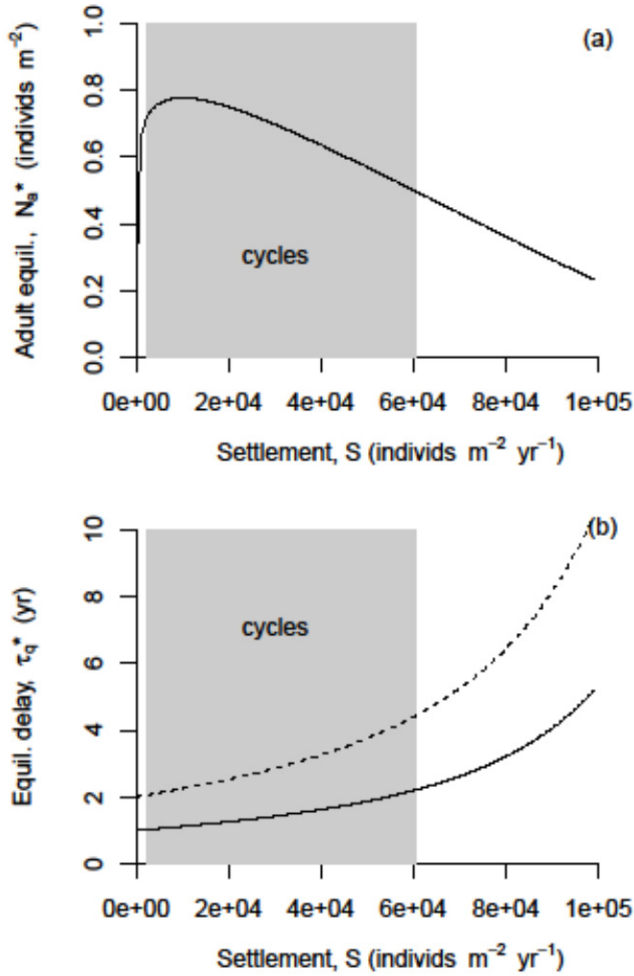


FIG. B7. Equilibrium (a) adult density, and (b) development delay for the model with heterogeneous larvae and  $p_h=0.5$ . In (b), the solid line indicates the delay for high quality larvae ( $\tau_h^*$ ), and the dashed line indicates the delay for low quality larvae ( $\tau_l^*$ ). This plot corresponds to a vertical cross-section through Fig. 2a (in the main text) at  $p_h=0.5$ . The model predicts an unstable point equilibrium with stable limit cycles for the range of  $S$  indicated by shading. The equilibrium is stable for larger and smaller values of  $S$ .

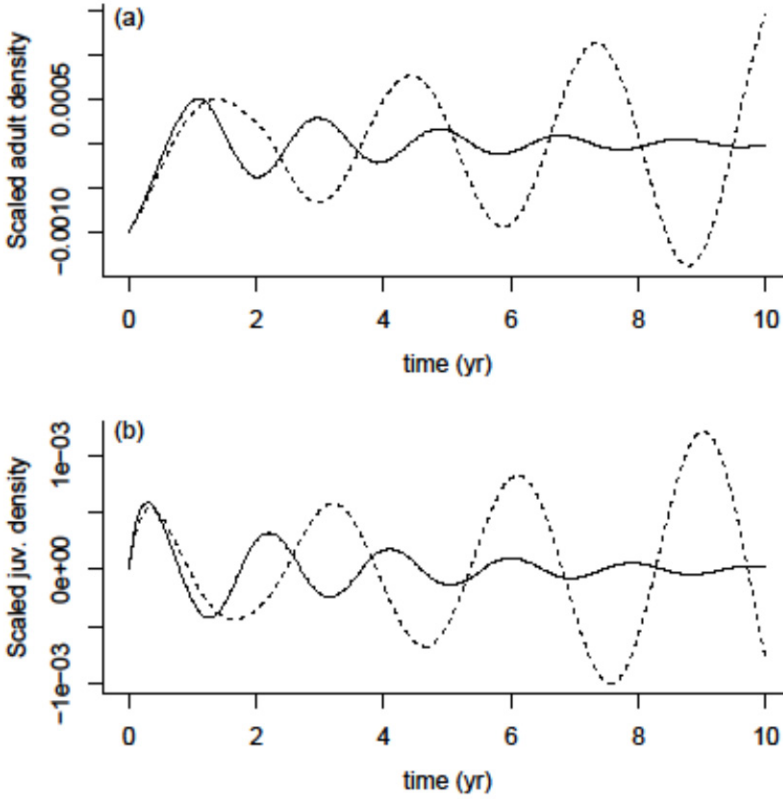


FIG. B8. Dynamics of (a) scaled adult density,  $\ln(N_a(t)/N_a^*)$ , and (b) scaled total juvenile density,  $\ln\left(\frac{N_{jh}(t)+N_{jl}(t)}{N_{jh}^*+N_{jl}^*}\right)$ . Solid lines represent dynamics in the stable region, with  $p_h=0.1$ .

Dashed lines represent dynamics in the unstable region, with  $p_h=10^{-6}$ . In both cases, settlement is  $S=10^3$  individuals  $m^{-2} yr^{-1}$ .

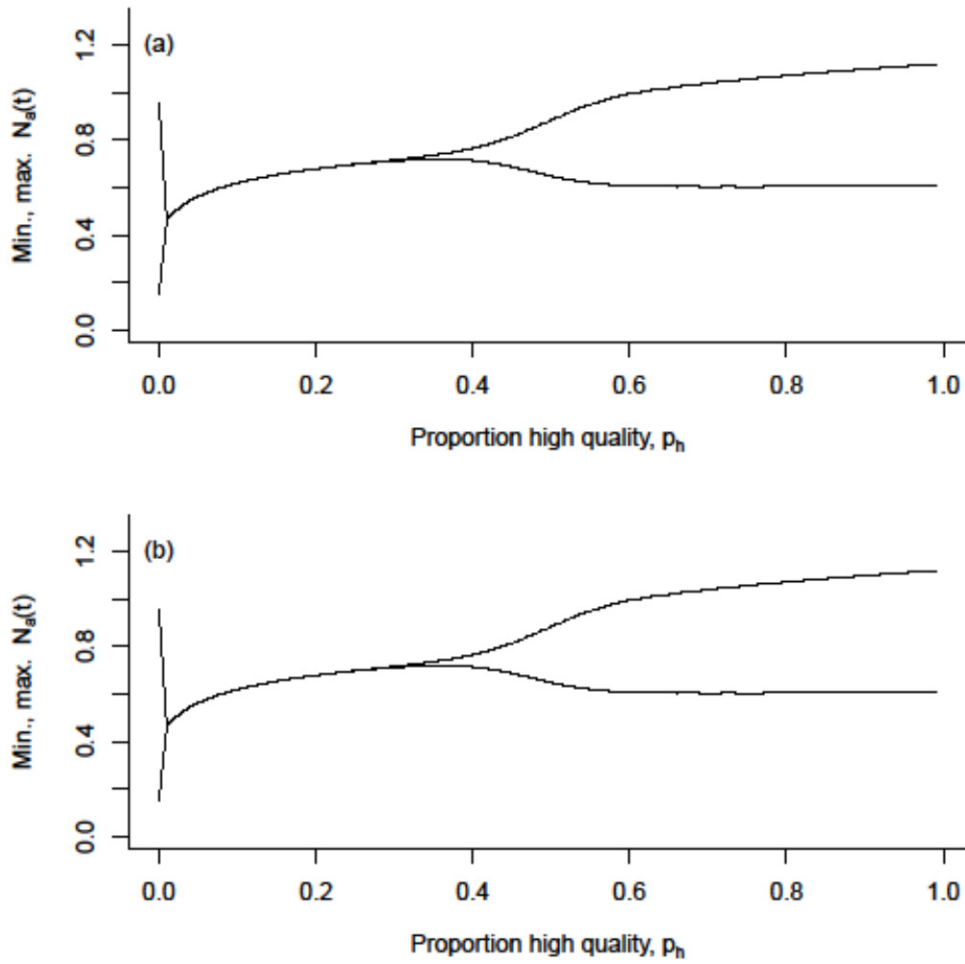


FIG. B9. Minimum and maximum adult densities,  $N_a(t)$ , on limit cycles predicted for two values of settlement rate: (a)  $S=10^4$ , and (b)  $S=5000$ . The equilibrium densities are stable and no limit cycles exist over the range of  $p_h$  where one line is present.

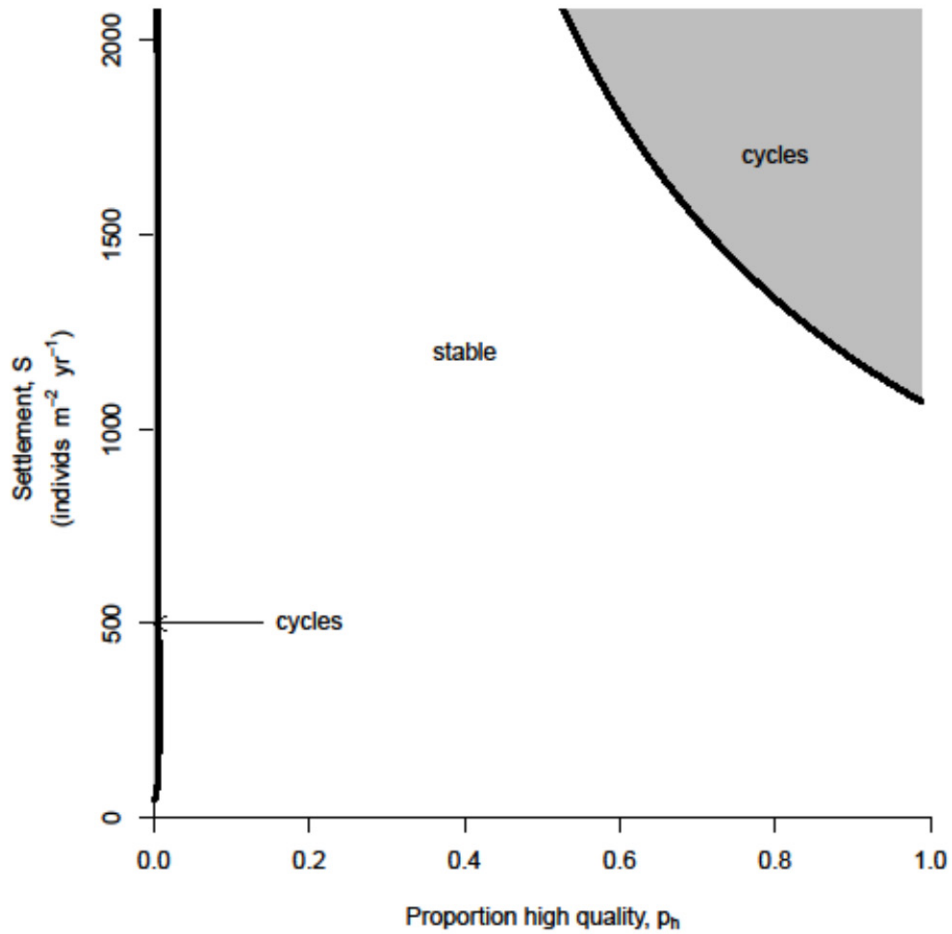


FIG. B10. Stability boundaries for low  $S$ , i.e., the lower portion of Fig. 2a. The equilibrium is stable at low  $S$  for any proportion high quality settlers,  $0 \leq p_h \leq 1$ . For extremely low and high values of  $p_h$ , the equilibrium is unstable for intermediate  $S$  (see Fig. 2a for upper stability boundaries).